Heating Mechanisms (Reconnection and Waves)

M. Asgari-Targhi
Harvard-Smithsonian Centre for Astrophysics

The Sun's Upper Atmosphere

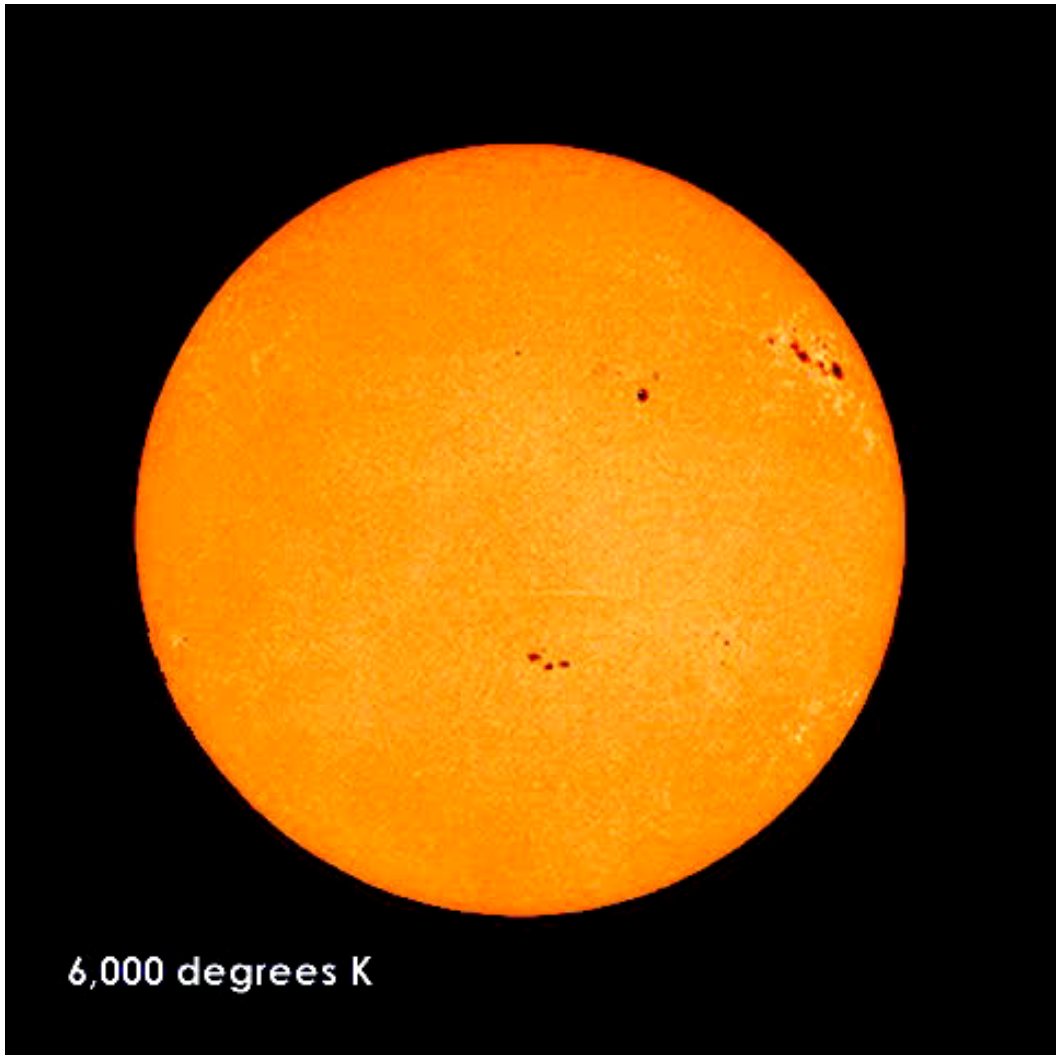

Coronal Loops

Coronal loops connect regions with opposite magnetic polarity in the photosphere. The X-ray emission from loops is highly variable:

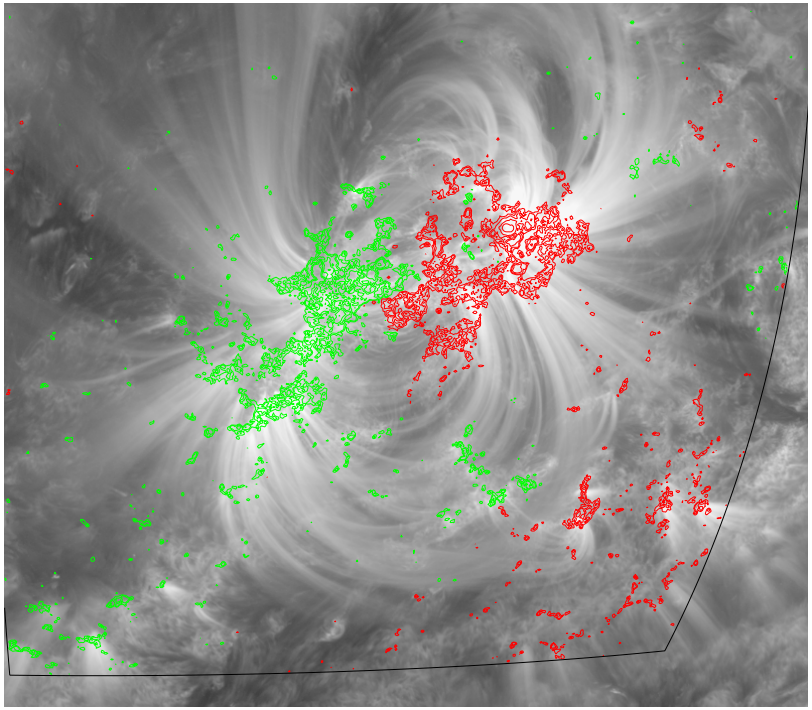

SDO observation of an active region NOAA 11564 on 2012 September 7 at 7:20 UT. The background image is from AIA 171 Å channel. Red and green contours indicate magnetic flux distribution based on the HMI magnetogram.

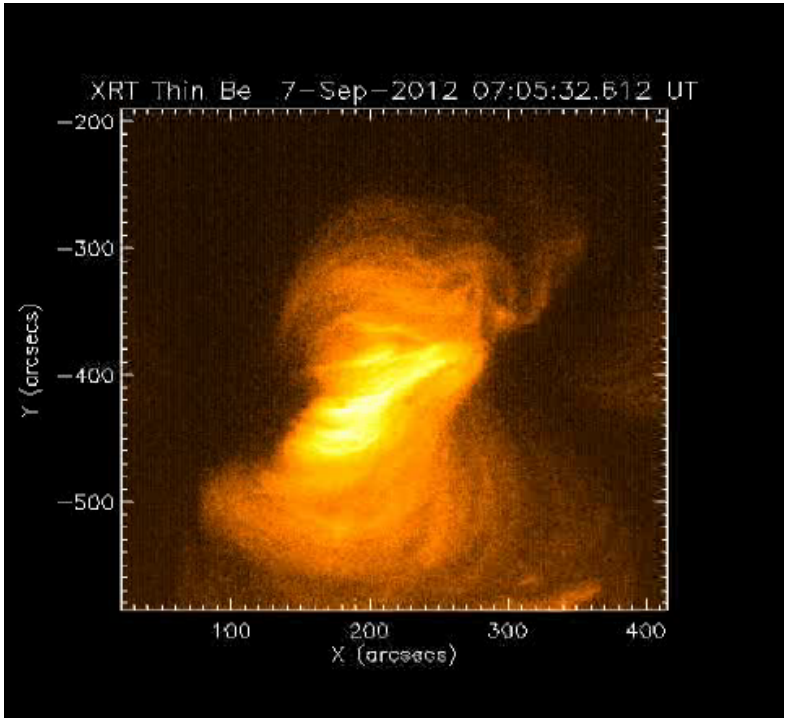

Display of coronal loops in the same active region (XRT/Hinode).

Photospheric Footpoint Motions

The source of energy for coronal heating lies in the Sun's convection zone:

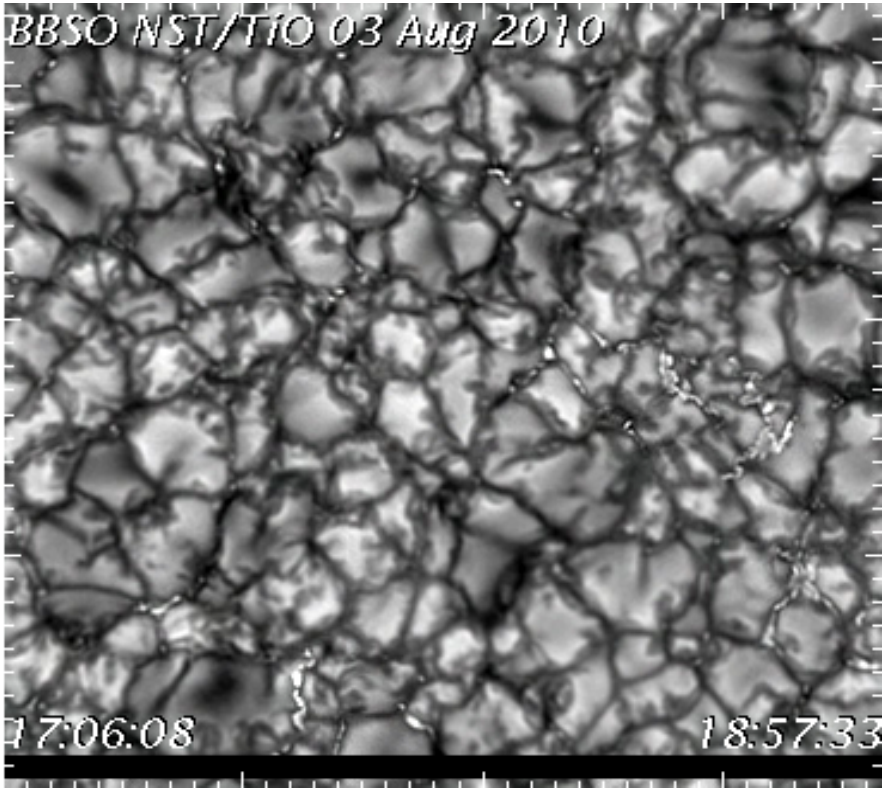

From: Big Bear Solar Observatory

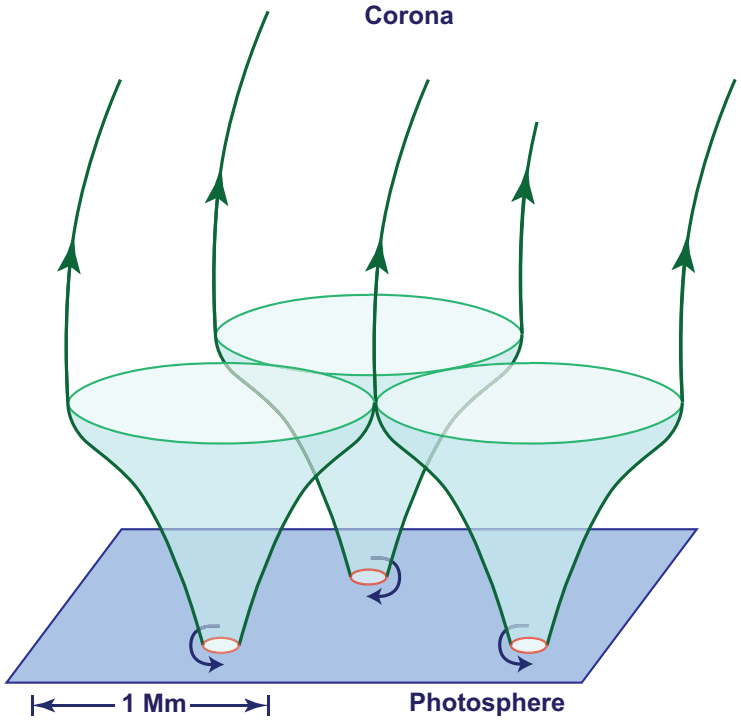

Horizontal flows cause transverse motions of magnetic elements in the photosphere, launching Alfven waves and creating field-aligned electric currents.

Chromosphere

- Spectral lines Ca II H & K are formed in the chromosphere:
- Magnetic regions are bright in these lines, indicating that magnetic field plays an important role in chromospheric heating.
- It is characterized by spicules, jet like features.
- Spicules are responsible for the transfer of mass and energy to the Chromosphere and corona (De Pontieu et al. 2007).

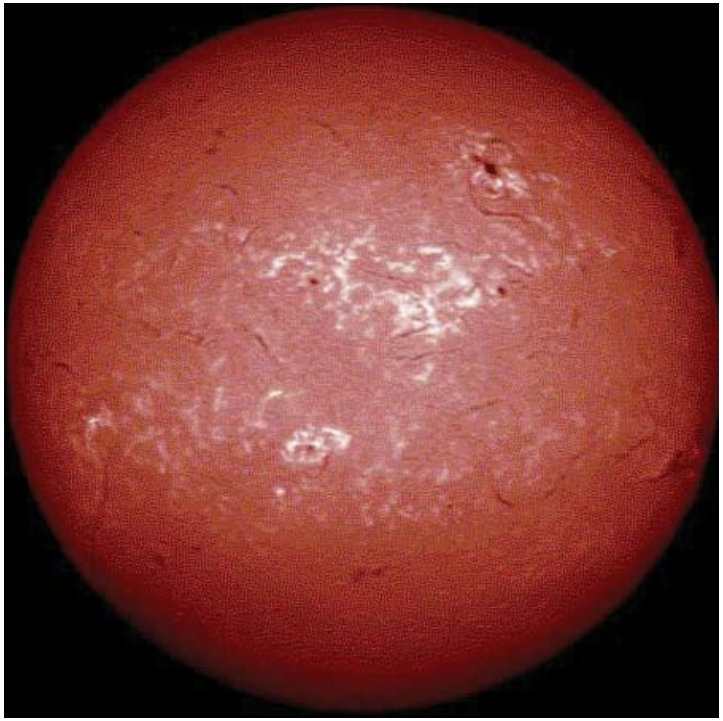

Chromosphere observed in H-alpha emission (credit Marshall Space Flight Center /NASA).

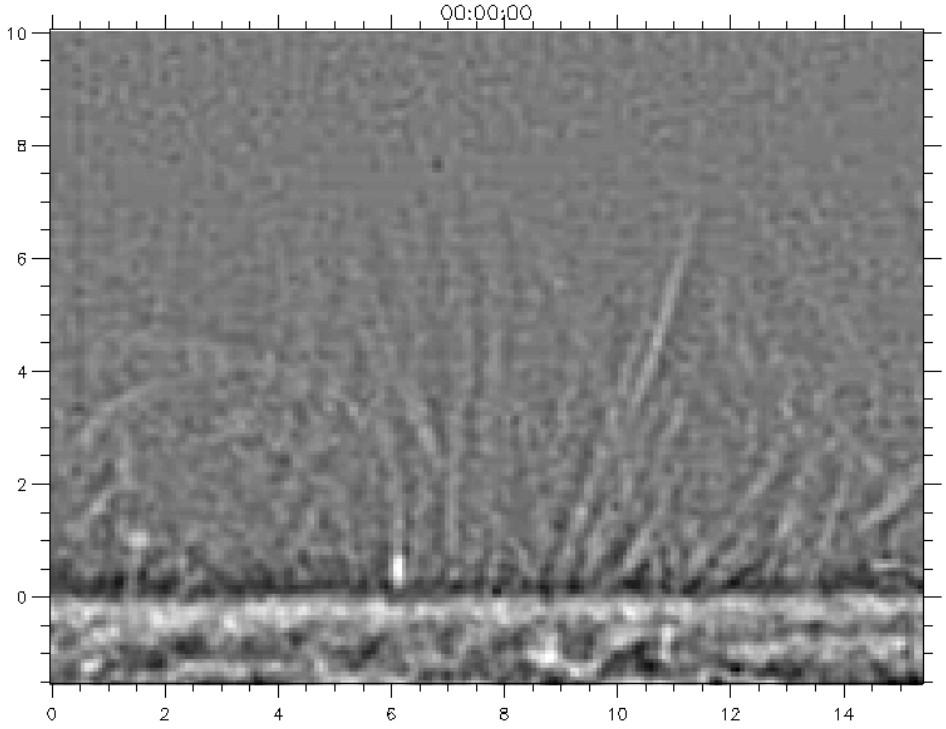

Temporal evolution of spicules (Hinode SOT in Ca II H 3968 Å filtergrams). The short-lived nature of the spicules is very apparent.

AC and DC Heating Models

- Stressing Models or DC Heating Models:

Energy is released from coronal magnetic fields that are stressed by slow random footpoint motions.

- Wave heating or AC Heating Models:

Heating results from the generation and dissipation of upwardly propagating waves.

- Key difference between DC and AC models:

Time scale τ_f of the footpoint motions in comparison to the coronal Alfven travel time L_{cor}/v_A.

- DC models: $\tau_f \gg L_{cor}/v_A$

  The corona has time to relax to an equilibrium state

- AC models: $\tau_f < L_{cor}/v_A$,

  Corona responds in a wave-like manner to the footpoint motions

The DC Heating Models

- Parker (1972, 1983) proposed that coronal loops are heated by dissipation of twisted/braided magnetic fields.
- Braids are produced by small-scale, random footpoint motions.
- The corona is assumed to respond *quasi-statically* to footpoint motion (sequence of force-free fields).
- Smooth equilibria scarce or nonexistent, for non-trivial topologies-current sheets must form.
- These current layers may either burn slowly (e.g., tearing modes), or burn quickly in a series of reconnection events or "nanoflares" (Parker 1988).

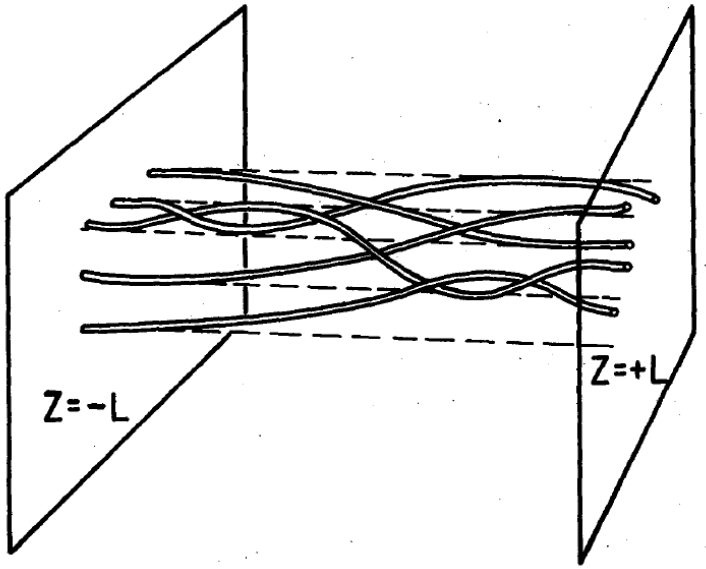

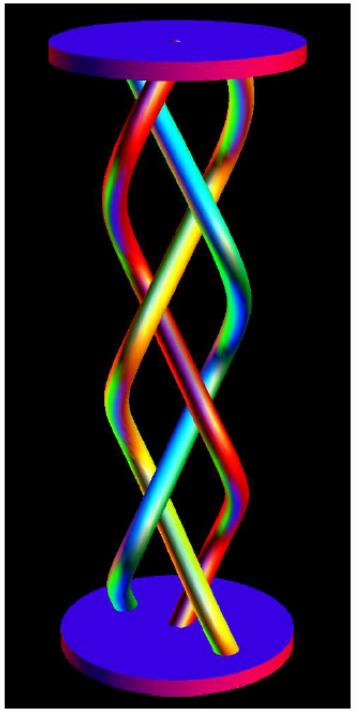

Current Sheets

Numerical simulations of magnetic braiding and the formation of tangential discontinuity (Wilmot-Smith et al. 2009a , 2009b, Ng & Bhattacharjee 1998 ; Janse & Low 2009 ; Low 2010 ; Janse et al. 2010 ; Craig 2010).

- Current sheets characterize the dissipative structure of the braided field lines.
- Current sheets are associated with magnetic reconnection giving rise to impulsive "bursty" heating events at the small scales (Rappazzo et al. 2008).

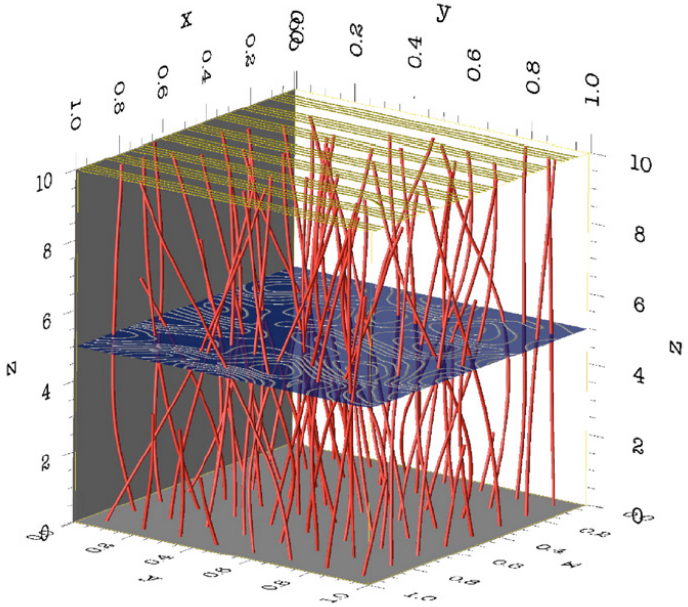

Transverse magnetic field lines (red)

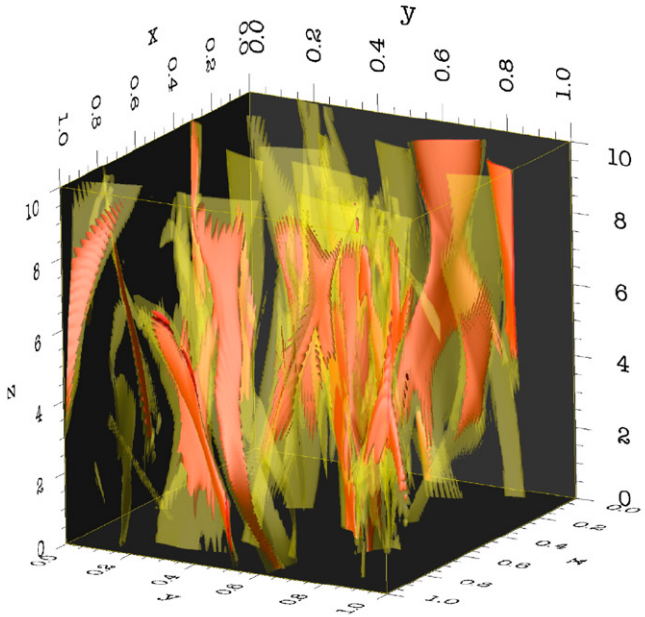

Current Sheets

Nanoflares

- The response of coronal loops to nanoflares has been studied in great detail

(e.g., Cargill 1994, Cargill & Klimchuk 1997 ; Winebarger & Warren 2005 ; Patsourakos & Klimchuk 2006 ; Klimchuk et al. 2008 ; Reep et al. 2013).

- Solar active regions may be heated by nanoflare storms.

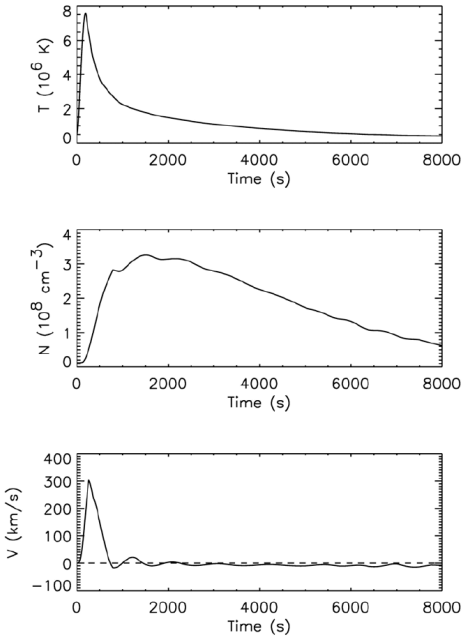

Spatially-averaged temperature, density, and velocity versus time for a loop strand that has been impulsively heated by a 500 s nanoflare (Klimchuk 2006).

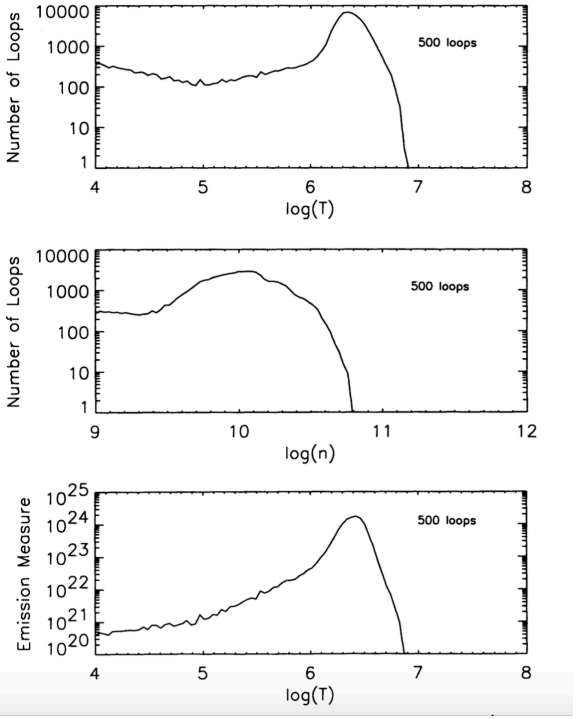

Evolution of 500 loops over a period of 10,000 seconds comprising of 3200 nanoflares (Cargill 1994).

Observational Evidence of Braided Field Lines

- Early observations of coronal loops do not show clear evidence of magnetic braiding (Schrijver 1999).
- Images from the High-resolution Coronal Imager (Hi-C) that was launched on a sounding rocket on 11th July 2012.
- HIC observed the corona in the 193A passband with a spatial resolution of about 0.2 arcsec (Cirtain et al. 2013).
- Authors claim to see highly braided magnetic fields at several locations in the observed active region.

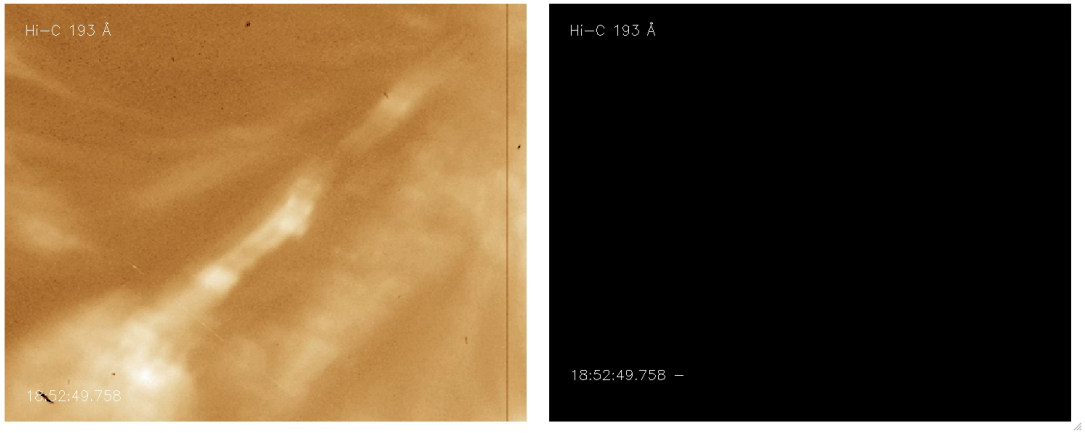

Hi-C 193 Å and AIA 193 Å data; the right panel shows a running difference movie (Cirtain 2013).

Evidence in Favour of DC heating Mechanism

- Mandrini et al. 2000 used Observations of coronal loops in soft X-rays.

- Found that models involving the gradual stressing of magnetic fields are generally in better agreement with the observations than are wave heating models (also see Demoulin et al. 2003).

TABLE 5

SUMMARY OF THE SCALING LAW FOR DIFFERENT MODELS OF CORONAL HEATING

Model Characteristics	N^0	References	Scaling Law	Parameters
Stressing Models (DC)				
Stochastic buildup	1	1	$B^2L^{-2}V^2\tau$	
Critical angle	2	2	$B^2L^{-1}V\tan\theta$	
Critical twist	3	3	$B^2L^{-2}VR\phi$	
Reconnection $\propto v_A$	4	4	$BL^{-2}\rho^{1/2}V^2R$	
Reconnection $\propto v_{A\perp}$	5	5	$B^{3/2}L^{-3/2}\rho^{1/4}V^{3/2}R^{1/2}$	
Current layers	6	6	$B^2L^{-2}V^2\tau\log R_m$	
	7	7	$B^2L^{-2}V^2\tau S^{0.1}$	
	8	8	$B^2L^{-2}V^2\tau$	
Current sheets	9	9	$B^2L^{-1}R^{-1}V_{ph}^2\tau$	
Taylor relaxation	10	10	$B^2L^{-2}V_{ph}^2\tau$	
Turbulence with:				
Constant dissipation coefficients	11	11	$B^{3/2}L^{-3/2}\rho^{1/4}V^{3/2}R^{1/2}$	
Closure	12	12	$B^{5/3}L^{-4/3}\rho^{1/6}V^{4/3}R^{1/3}$	
Closure + spectrum	13	13	$B^{s+1}L^{-1-s}\rho^{(1-s)/2}V^{2-s}R^s$	$s=0.7, m=-1.$
	14			$s=1.1, m=-2.5$
Wave Models (AC)				
Resonance	15	14	$B^{1+m}L^{-3-m}\rho^{-(1+m)/2}$	$m=-1.$
	16			$m=-2.$
Resonant absorption	17	15	$B^{1+m}L^{-1-m}\rho^{-(1+m)/2}$	$m=-1.$
	18			$m=-2.$
	19	16	$B^{1+m}L^{-m}\rho^{-(m-1)/2}$	$m=-1.$
	20			$m=-2.$
Current layers	21	17	$BL^{-1}\rho^{1/2}V^2$	
Turbulence	22	18	$B^{5/3}L^{-4/3}R^{1/3}$	

REFERENCES.—(1) Sturrock & Uchida 1981, Berger 1991; (2) Parker 1988, Berger 1993; (3) Galsgaard & Nordlund 1997; (4) Parker 1983; (5) Parker 1983, modified; (6) van Ballegooijen 1986; (7) Hendrix et al. 1996; (8) Galsgaard & Nordlund 1996; (9) Aly & Amari 1997; (10) Heyvaerts & Priest 1984, Browning & Priest 1986, Vekstein et al. 1993; (11) Einaudi et al. 1996, Dmitruk & Gómez 1997; (12) Heyvaerts & Priest 1992, Inverarity et al. 1995, Inverarity & Priest 1995a; (13) Milano et al. 1997; (14) Hollweg 1985; (15) Ofman et al. 1995, Ruderman et al. 1997; (16) Halberstadt & Goedbloed 1995; (17) Galsgaard & Nordlund 1996; (18) Inverarity & Priest 1995b.

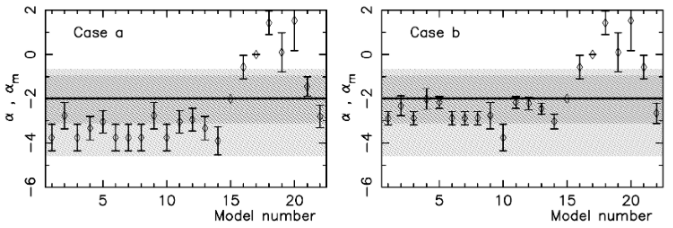

FIG. 8.—Comparison of the heating rate vs. length scaling law, $H \propto L^{\alpha}$, as deduced from observations and models. The plotted points with error bars indicate the power-law index α_m predicted by the models listed in Table 5. The horizontal line at $\alpha = -2$ is the most probable value deduced from observations (Porter & Klimchuk 1995), with the dark (light) shaded band representing the 90% confidence interval associated with the pressure (temperature) measurements.

Evidence in Favor of DC heating Mechanism

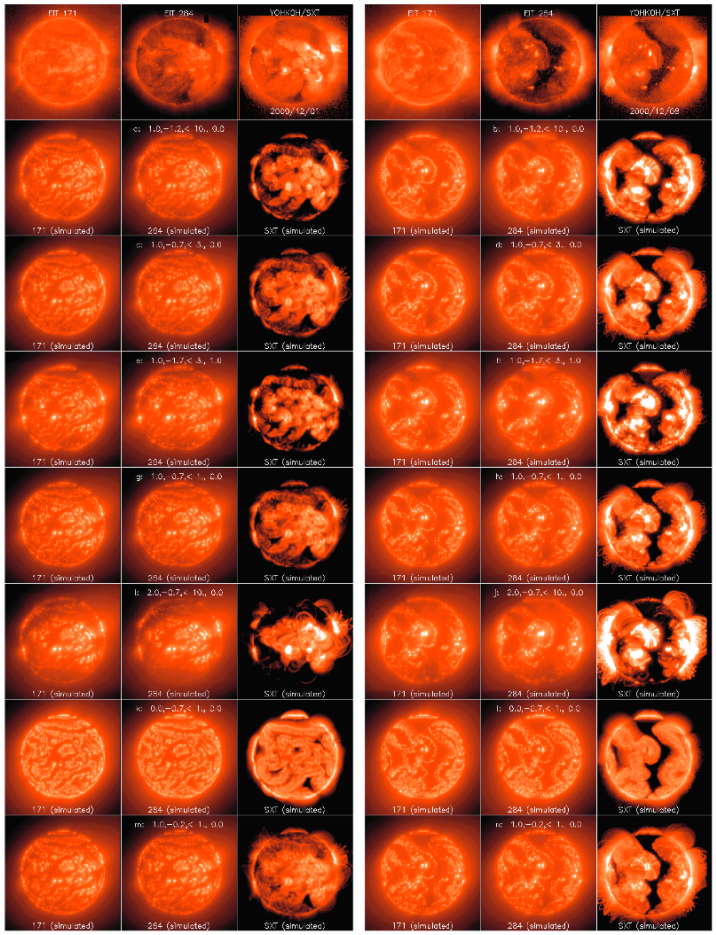

Observed and simulated images of the solar corona for 1st of December 2000. The observed images (top row) for EIT 171 Å, EIT 284 Å and Al/Mg SXT. Seven sets of simulated images follow, with the best-fit case on the second row (Schrijver et al. 2004).

- Schrijver & Aschwanden (2002) and Schrijver et al. (2004) simulated the appearance of the solar corona in various wavelength bands, using different assumed heating mechanisms.
- The best match to the X-ray and EUV observations was obtained for an energy flux F_H into the corona given by $F\_H \approx 4 \times 10^{14}\, B/L_h$ (in erg cm^{-2} s^{-1}), where *B* is the magnetic field strength at the chromospheric base (in G) and L_h is the loop half-length.
- Based on this B/L_h scaling, Schrijver et al. (2004) concluded that DC reconnection at tangential discontinuities is the most likely mechanism for coronal heating.
- However, this modeling did not describe in detail how the energy is injected into the corona.

Reconnection

In some versions of the braiding model the reconnection switches on when the misalignment angle between neighboring flux tubes reaches a critical value resulting in a nanoflare (Parker 1988 ; Berger 1993 ; Dahlburg et al. 2005).

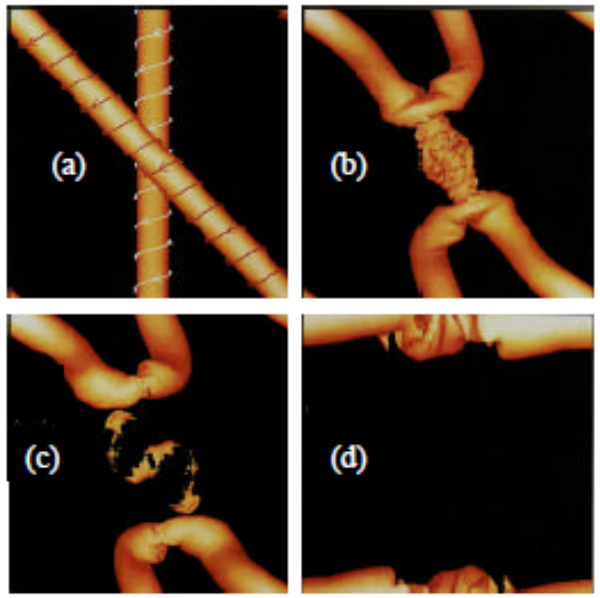

Linton, Dahlberg and Antiochos 2001.
Dahlburg, Klimchuk & Antiochos 2005.

Reconnection

- In other versions of DC heating models, the reconnection occurs even for small angles (van Ballegooijen 1986).

Braiding leads to a cascase of magnetic energy to small transverse scales, where the energy is dissipated (van Ballegooijen 1985, 1986).
Predicted heating rate (per unit volume):

$$Q_{cor} \approx \frac{B_0^2}{8\pi} \frac{2u_0^2 \tau_0 \ln R_m}{3L^2\sqrt{2\pi}},$$

where B_0 is coronal field strength, L is loop length,
u_0 is footpoint velocity, τ_0 is correlation time.
Note: heating is proportional to the "diffusion constant" of the footpoint motions, $D \approx u_0^2 \tau_0$.
Using $D \approx 250$ km^{2}s^{-1} (DeVore et al. 1985), it was found that heating rate predicted by cascase model is too small by factor 10 to 40.

Numerical Models of Magnetic Braiding

- Models with realistic 3D MHD models of active regions (e.g., Gudiksen & Nordlund 2002, 2005a, 2005b; Bingert & Peter 2011, 2013; Peter & Bingert 2012; Bourdin et al. 2013).
- These models include the effects of the lower atmosphere,
- Predict that the corona responds almost quasi- statically to the footpoint motions, and that the coronal heating is dominated by the dissipation of field-aligned electric currents (e.g., Bingert & Peter 2011).

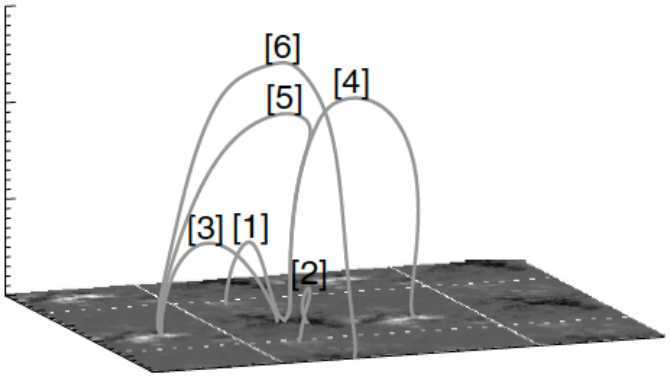

3D representation of six magnetic field lines (Bingert & Peter 2011)

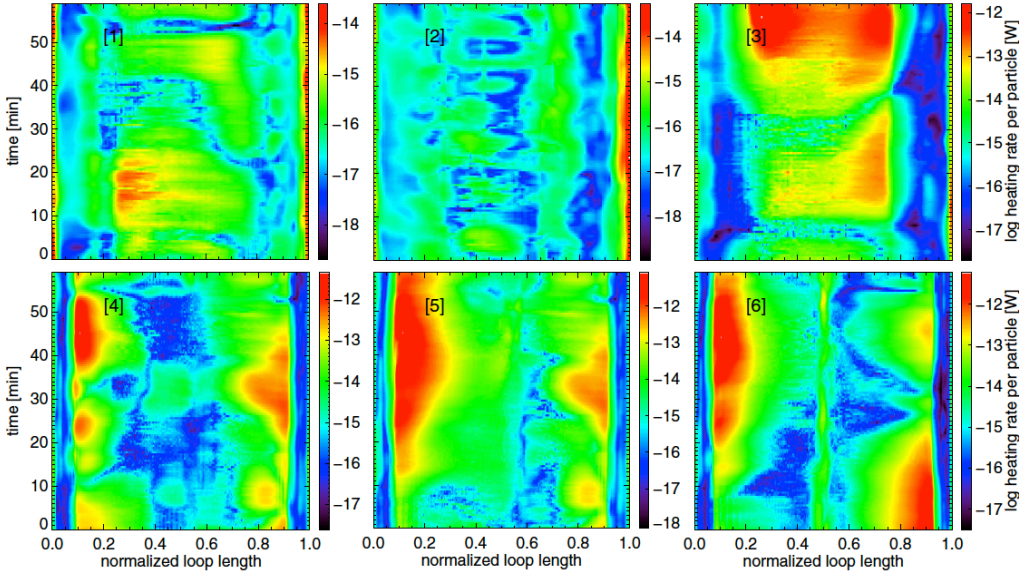

Heating rate per particle (Bingert & Peter (2011)).

Numerical Models of Magnetic Braiding

- In simulation by Bingert & Peter (2011) the energy flux into the corona is only about 10^5 erg cm^{-2} s^{-1} (Figure 1).
- The horizontally averaged coronal temperature is less than 1 MK (Figure 2), whereas observed active regions have energy fluxes of about 10^7 erg cm^{-2} s^{-1} (Withbroe & Noyes 1977) and temperatures in the range 3–5 MK.

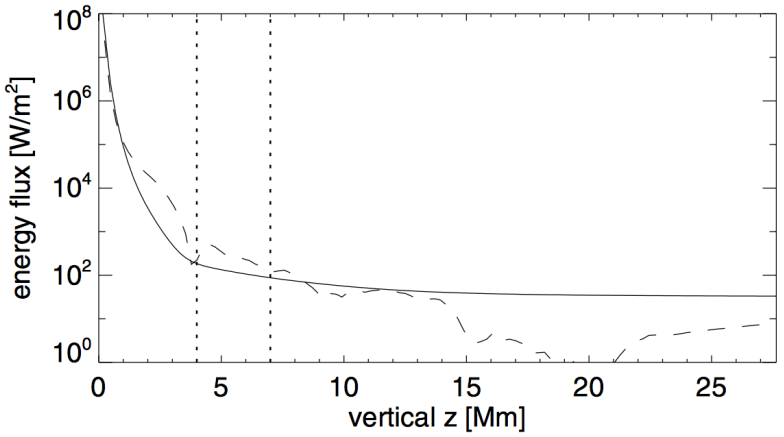

Figure1. Energy flux as a function of height.

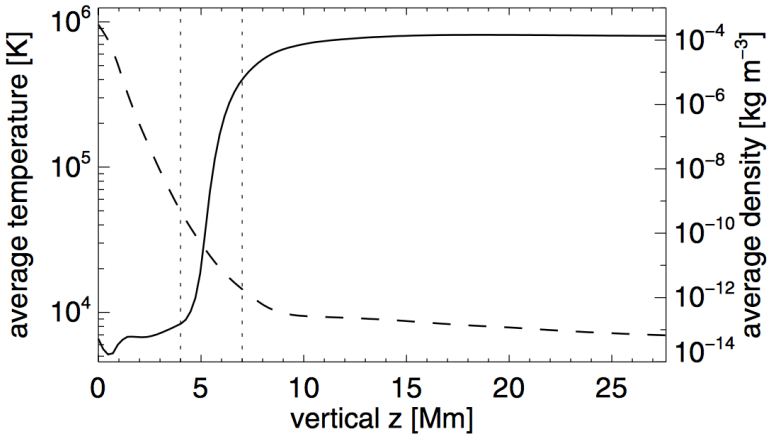

Figure2. Horizontally averaged temperature (solid) and density (dashed) over height for one snapshot.

- To boost the temperature from 1 MK to 3 MK requires a significant increase in the heating rate (by a factor ~47).

Coronal Heating Models

- Inherent in Parker's analysis is :

The assumption that coronal magnetic flux tubes Can be wrapped around each other over a period of many hours, i.e., the flux tubes must retain their identity for a long time.

- This assumption is questionable since observations have shown that photospheric flux elements continually split up and merge on a timescale of a few minutes (Berger & Title 1996).

- Time series of G band images taken from an area of an active region. Times are UT and increase in column from upper left.

- Changes to the central bright point due to the interaction of the flux element with convective flow field.

- After a flux element breaks up, the individual fragments disperse as a consequence of turbulent motions below the photosphere. It is not clear what effect this will have on the process of coronal heating.

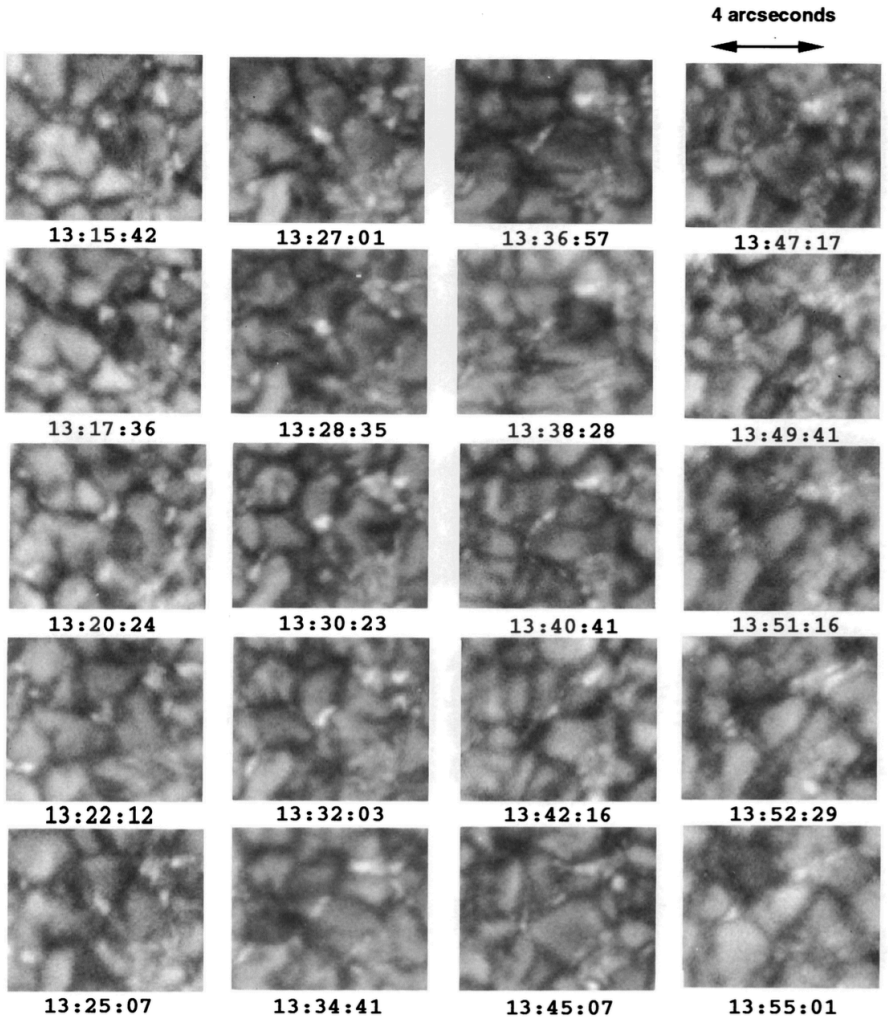

Waves Heating Models

- Alfven waves have received particular attention because of their ability to transport energy over different layers of the solar atmosphere.
- Motions are imposed at the *photospheric* footpoints, not the base of the corona.
- Alfvén waves are driven by motions *inside* the photospheric flux elements.

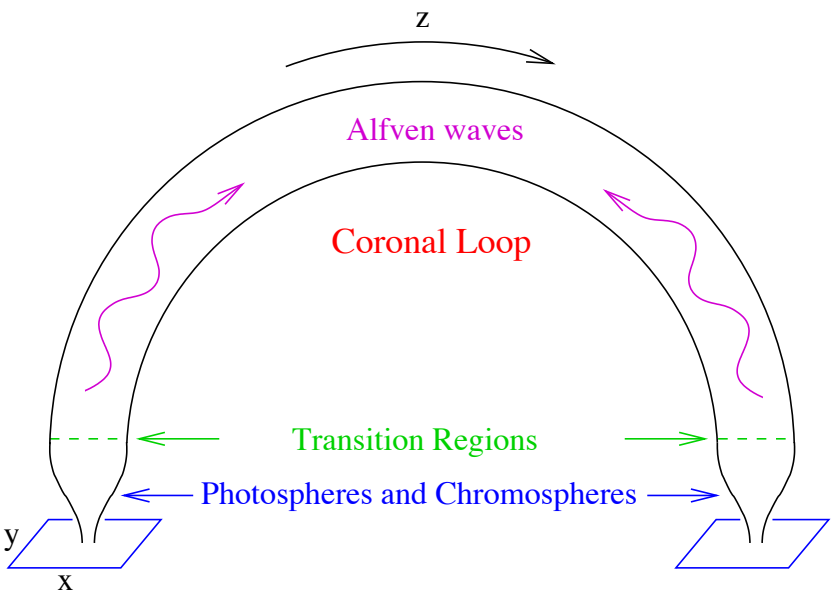

Waves Heating Models

Different mechanisms for the dissipation of the Alfven waves :

- phase mixing and resonant absorption

(Heyvaerts & Priest 1983; De Groof & Goossens 2002; Goossens et al. 2011).

- turbulent cascade of wave energy

(e.g., Hollweg 1986; Gomez & Ferro Fontan 1988; Heyvaerts & Priest 1992; Milano et al. 1997; Chae et al. 1998; Matthaeus et al. 1999; Verdini & Velli 2007; Cranmer et al. 2007, van Ballegooijen et al. 2011).

- coupling with compressive wave modes

(Kudoh & Shibata 1999; Moriyasu et al. 2004; Suzuki & Inutsuka 2006; Antolin et al. 2008; Antolin & Shibata 2010; Matsumoto & Shibata 2010).

Alfven Wave Turbulence Model

Simulations of Alfven waves in coronal loops (van Ballegooijen at al. 2011, Asgari & van Ballegooijen 2012):

- Alfven speed increases with height in lower atmosphere.
- Background temperature and Alfven speed as functions of position for an observed loop.

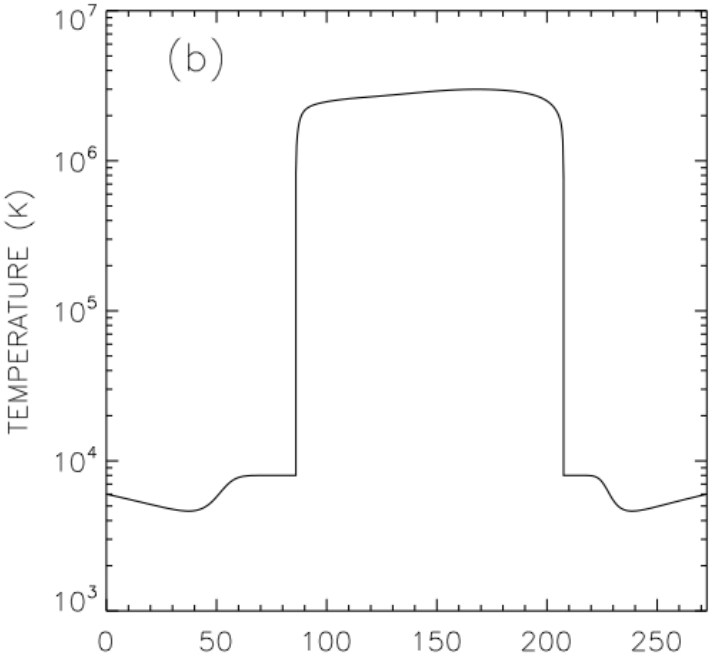

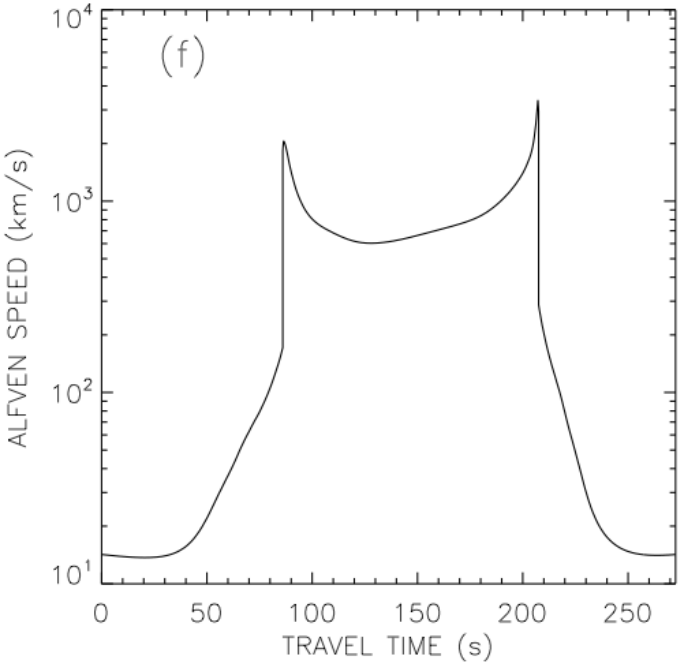

Alfven Wave Turbulence Model

- Waves strongly reflect at the transition region (TR), creating Counter-propagating waves in the chromosphere.
- Nonlinear interactions between counter-propagating waves lead to turbulence in the chromosphere and the corona.
- Small fraction of wave energy is transmitted through TR into the corona, producing turbulence there.
- The waves that enter the corona have been modified by chromospheric turbulence.
- All of the above have the effect of producing braided field lines in the corona.

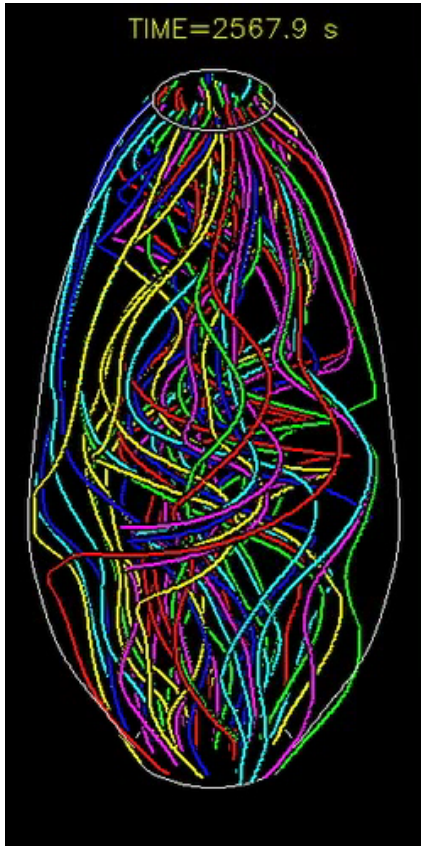

Time dependent model of braiding (van Ballegooijen et al. 2014)

Alfven Wave Turbulence Model

- Predicted rms velocities (left) are consistent with observed spectral line widths from EIS
- Heating rate in the choromosphere and the corona

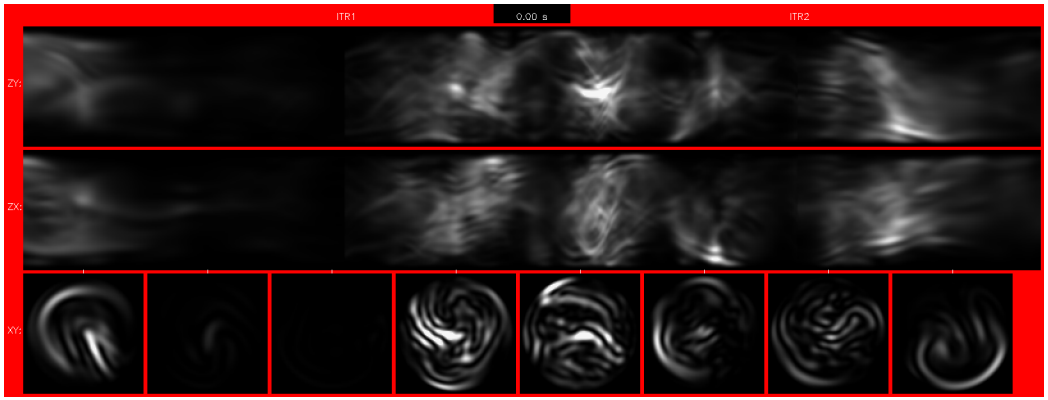

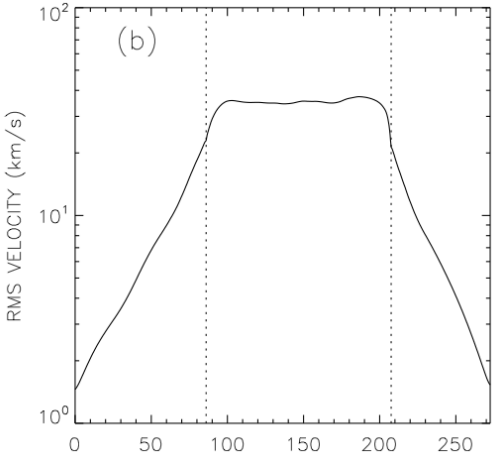

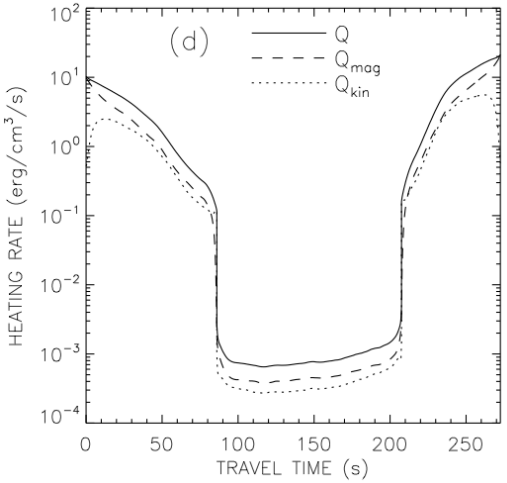

Non-thermal Line Width from EIS

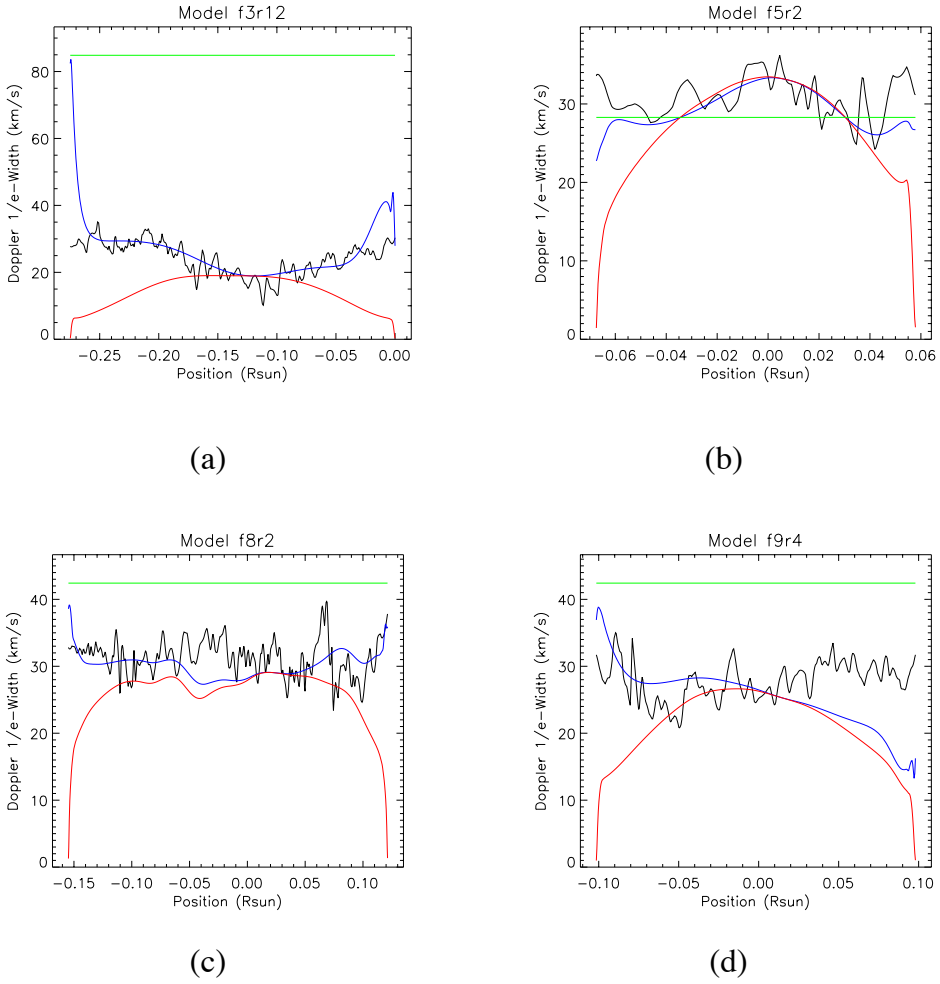

Non-thermal line widths in Fe XII λ192.394 for four field lines (Asgari et al. 2014)

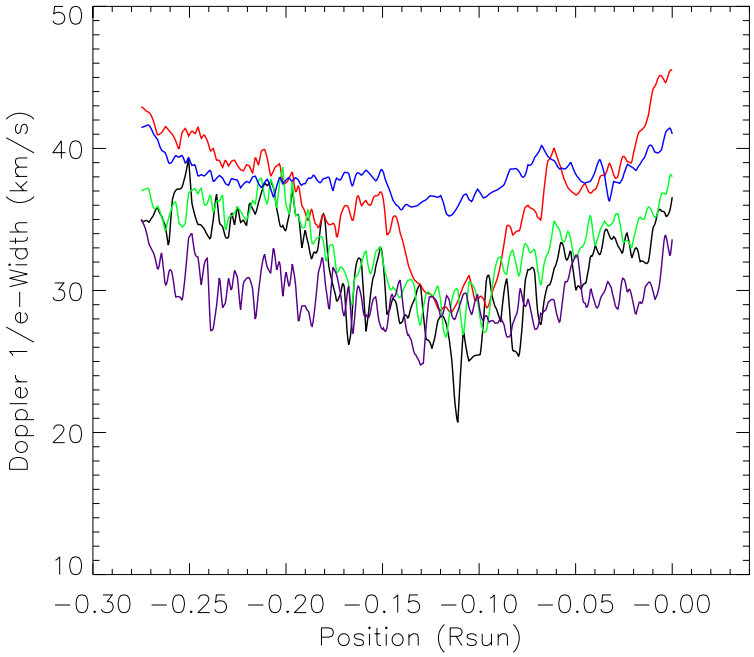

Non-thermal line widths of the observed spectral lines as function of position s along the path of a field line.

Fe XII λ192.394 black solid line
Fe XII λ195.119 red
Fe XIII λ202.044 green
Fe XV λ284.160 blue
Fe XVI λ262.980 purple

- Note that for most lines the width has its largest values near the ends of the coronal loop

Spicules

- Jets and spicules dominate the region between the chromosphere and corona.
- Spicules are associated with swaying motions and parallel flows.
- They maybe responsible for creating field aligned flows along the magnetic field lines.
- Hence, transporting mass and energy from the chromosphere to the corona.

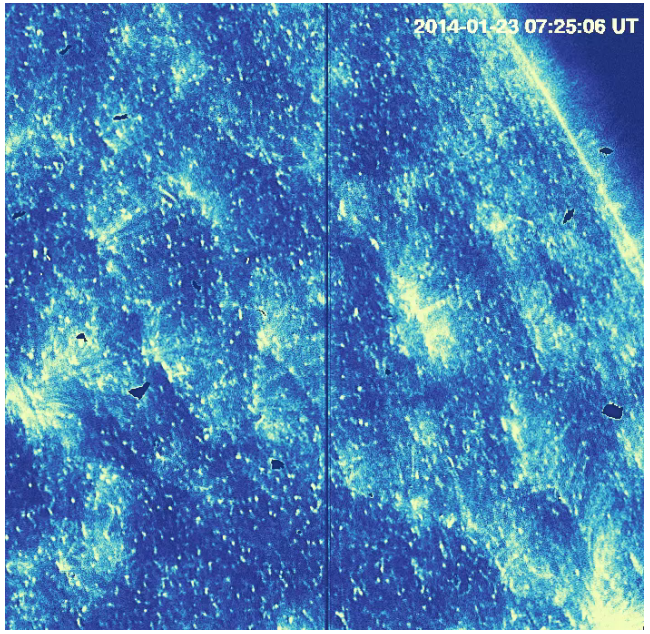

Transition region network jets. Some are likely on disk counterparts and heated parts of the spicules observed with IRIS (Tian et al. 2014).

Discussions

The Alfven Wave Turbulence (AWT) model has several advantages over DC heating models:

- The energy dissipation rates predicted for active region loops are sufficient to explain the observed coronal temperatures, while for DC models the heating rates fall short by at least one order of magnitude.

- The AWT model predicts small perturbations in the directions of the coronal magnetic field (misalignment angles ~4 degrees).

- The AWT models are consistent with the non- thermal velocities derived from observed spectral line widths.

Conclusions

- The basic problem in DC models is that the transverse velocities at the coronal base are similar to the those in the photosphere (only a few km/s), but much higher velocities are needed to heat the corona to temperatures in the range 3–5 MK.

- In DC models, the transverse velocities at the coronal base are similar to those at the photospheric footpoints, too small to explain the observed line widths.

- At present the spatial resolution of some of the DC models (Binger and Peter 2011) is ~200 km.

- This is not sufficient to simulate Alfven Waves that require a much higher resolution.

- As the resolution of these models is further increased, the magnetic perturbations may become more wave-like and the heating may be dominated by AC processes.